Role of the πσ* State in Molecular Photophysics

ARTICLE *in* ACCOUNTS OF CHEMICAL RESEARCH · APRIL 2010

Impact Factor: 22.32 · DOI: 10.1021/ar9002043 · Source: PubMed

3 AUTHORS:

Marek Zgierski
National Research Council Canada
340 PUBLICATIONS **8,215** CITATIONS
SEE PROFILE

Takashige Fujiwara
The Ohio State University
39 PUBLICATIONS **523** CITATIONS
SEE PROFILE

Edward Lim
University of Akron
99 PUBLICATIONS **1,584** CITATIONS
SEE PROFILE

Role of the πσ* State in Molecular Photophysics

Zgierski, Marek Z.; Fujiwara, Takashige; Lim, Edward C.

Publisher's version / la version de l'éditeur:
Accounts of Chemical Research, 43, 4, pp. 506-517, 2010-01-15

Web page / page Web
http://dx.doi.org/10.1021/ar9002043
http://nparc.cisti-icist.nrc-cnrc.gc.ca/npsi/ctrl?action=rtdoc&an=17673496&lang=en
http://nparc.cisti-icist.nrc-cnrc.gc.ca/npsi/ctrl?action=rtdoc&an=17673496&lang=fr

ACCOUNTS
of chemical research

Role of the $\pi\sigma^*$ State in Molecular Photophysics

MAREK Z. ZGIERSKI,[†] TAKASHIGE FUJIWARA,[‡] AND EDWARD C. LIM*[,‡,§]

[†]*Steacie Institute for Molecular Science, National Research Council of Canada, Ottawa K1A 0R6, Canada and,* [‡]*Department of Chemistry and The Center for Laser and Optical Spectroscopy, The University of Akron, Akron, Ohio 44325-3601*

RECEIVED ON JULY 14, 2009

CONSPECTUS

Photosynthesis, which depends on light-driven energy and electron transfer in assemblies of porphyrins, chlorophylls, and carotenoids, is just one example of the many complex natural systems of photobiology. A fuller understanding of the spectroscopy and photophysics of simple aromatic molecules is central to elucidating photochemical processes in the more sophisticated assemblies of photobiology. Moreover, developing a better grasp of the photophysics of simple aromatic molecules will also enhance our ability to create and improve practical applications in photochemical energy conversion, molecular nanophotonics, and molecular electronics. In this Account, we present a concerted experimental and theoretical study of aromatic ethynes, aromatic nitriles, and fluorinated benzenes, illustrating the important roles that the low-lying $\pi\sigma^*$ state plays in the electronic relaxation of these aromatic compounds.

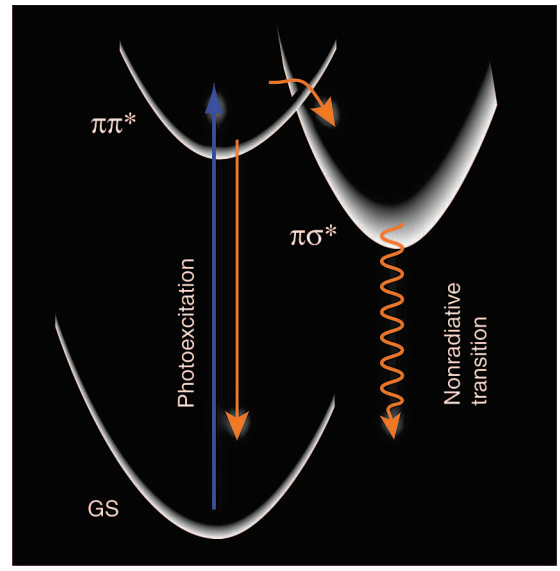

Diphenylacetylene, 4-dialkylaminobenzonitriles, 4-dialkylaminobenzethynes, and fluorinated benzenes exhibit fluorescence that strongly quenches as the excitation energy is increased for gas-phase systems and at elevated temperatures in solution. Much of this interesting photophysical behavior can be attributed to the presence of a dark intermediate state that crosses the fluorescent $\pi\pi^*$ state. Our quantum chemistry calculations, as well as time-resolved laser spectroscopies, indicate that this dark intermediate state is the $\pi\sigma^*$ state that arises from the promotion of an electron from the π orbital of the phenyl ring to the σ^* orbital localized in the C≡X group (where X is CH and N) or on the C—X group (where X is a halogen). These crossings not only lead to the strong excitation energy and temperature dependence of fluorescence but also induce highly interesting $\pi\sigma^*$-mediated intramolecular charge transfer in 4-dialkylaminobenzonitriles.

Most previous studies on the excited-state dynamics of organic molecules have examined aromatic hydrocarbons, nitrogen heterocycles, aromatic carbonyl compounds, and polyenes, which have low-lying excited states of $\pi\pi^*$ character (hydrocarbons and polyenes) or $n\pi^*$ and $\pi\pi^*$ character (carbonyls and N-heterocycles). These studies have revealed important involvement of selection rules (promoting vibrational modes and spin—orbit coupling) and Franck—Condon factors for radiationless transitions, which have important effects on photophysical properties. The recent experimental and time-dependent density functional theory (TDDFT) calculations of aromatic ethynes, nitriles, and perfluorinated benzenes described in this Account demonstrate the importance of the bound excited state of a $\pi\sigma^*$ configuration in these molecules.

Introduction

Spectroscopy and photophysics of simple aromatic molecules are central to the understanding of photochemical and photobiological processes in complex system of importance to life. Photosynthesis, which depends on the light-driven energy and

Published on the Web 01/15/2010 www.pubs.acs.org/acr
10.1021/ar9002043

electron transfer in assemblies of porphyrins, chlorophylls, and carotenoids, is a prime example of such complex systems. Apart from its fundamental importance, the photophysics of simpler aromatic molecules has practical applications in photochemical energy conversion, molecular nanophotonics, and molecular electronics.

Most of the past studies on the excited-state dynamics of organic molecules have been concerned with aromatic hydrocarbons, nitrogen heterocyclic compounds, aromatic carbonyl compounds, and polyenes, which possess low-lying excited states of $\pi\pi^*$ character (hydrocarbons and polyenes) or $n\pi^*$ and $\pi\pi^*$ character (carbonyls and N-heterocyclics).[1] The photophysics of these molecules has therefore been described and interpreted in terms of the low-lying $\pi\pi^*$ or $n\pi^*$ states. These studies, carried out over several decades, have revealed important involvement of selection rules (promoting vibrational modes and spin−orbit coupling) and Franck−Condon factors for radiationless transitions, which have important effects on the photophysical properties.

Recent computational and experimental studies on aromatic ethynes, aromatic nitriles, and fluorinated benzenes show that the bound excited state of a $\pi\sigma^*$ configuration, which arises from the promotion of an electron from the aromatic π orbital to the σ^* orbital, localized on the −C≡CH, −C≡N, or −C−F group, can be low-lying, and it has pronounced effects on the fluorescence of such compounds. More specifically, the fluorescence of diphenylacetylene or 4-dialkylaminobenzonitriles, generated at excitation energies above that of the emission threshold, is strongly quenched in the gas phase or at higher temperatures in solution. Quantum chemistry calculations as well as the time-resolved spectroscopies indicate that due to the greatly different geometry of the $\pi\sigma^*$ state relative to that of the fluorescent $\pi\pi^*$ state, the $\pi\sigma^*$ state crosses the fluorescent $\pi\pi^*$ state along the nuclear coordinate involving bending of the C≡CH and C≡N triple bonds. This crossing between the bright $\pi\pi^*$ state and the dark (or very weakly fluorescent) $\pi\sigma^*$ state can account for the fluorescence break-off (loss) at excitation energies higher than that needed to excite fluorescence in the gas phase and at higher temperatures in solution. Moreover, in the case of 4-dialkylaminobenzonitriles, the $\pi\sigma^*$ state plays a key intermediate role in inducing an intramolecular charge transfer (ICT).

In this Account, we describe the spectroscopy and photophysics of aromatic ethynes, nitriles, and perfluorinated benzenes in the gas phase and in solution and their rationalizations based on the time-dependent density functional theory (TDDFT) calculations.

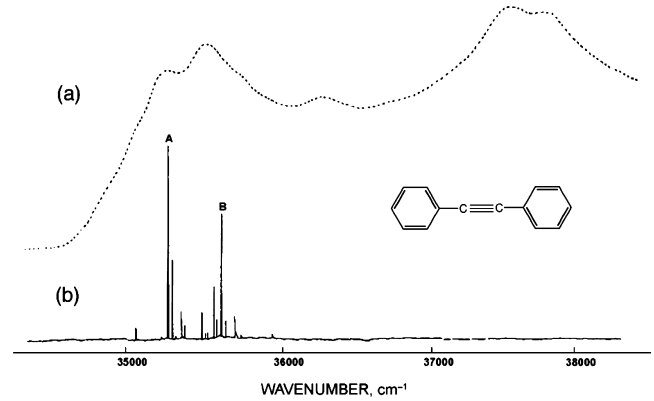

FIGURE 1. (a) Vapor absorption and (b) fluorescence excitation spectra of diphenylacetylene (DPA) in a supersonic free jet. Adapted with permission from ref 2.

Aromatic Ethynes

Diphenylacetylene, Di-2-thienylacetylene, and Di-2-furlacetylene. Our initial interest in the photophysics of aromatic ethynes began from the reading of the 1984 paper by Okuyama et al.[2] on the fluorescence excitation spectrum of diphenylacetylene (DPA) in the gas phase. Figure 1b presents the fluorescence excitation spectrum of the molecule they had measured under a supersonic jet expansion. The most remarkable feature of the spectrum is the abrupt break off (i.e., loss) of fluorescence that occurs for excitation energies exceeding about 500 cm^{-1} above the electronic origin of the S_1 (B_{1u}) ← S_0 (A_g) absorption, Figure 1a. This observation could be accounted for if a dark (nonfluorescent) electronic state intersects the emitting S_1 (B_{1u}) state at energy slightly above the potential minimum of the $\pi\pi^*$ state.

To probe the nature of the dark state leading to the anomalous photophysical properties of DPA, we have carried out time-dependent DFT (TDDFT), configuration interaction with singles (CIS), and complete active space self-consistent-field (CASSCF) calculations of the low-lying excited states of the molecule.[3] The results of these calculations, shown in Figure 2, indicate that while the lowest-energy excited singlet state is the B_{1u} ($\pi\pi^*$) state in linear D_{2h} symmetry, the nonfluorescent $\pi\sigma^*$ state of A_u symmetry is the lowest in energy in bent C_{2h} symmetry. This leads to the crossing of the fluorescent $\pi\pi^*$ state (B_u in C_{2h} point group) and the dark $\pi\sigma^*$ potential energy curves at a CCC (θ) angle of 148°. The presence of a small energy barrier for the state switch from the initially excited $^1B_{1u}$ ($\pi\pi^*$) state of linear geometry ($\theta = 180°$) to the dark $\pi\sigma^*$ state of bent geometry ($\theta = 120°$) can account for the loss of fluorescence in gas phase at higher excitation energy[2] and the thermally activated quenching of fluorescence in solution,[4] shown in Figure 3. Interestingly, the threshold temperature (>120 K) at which the thermal quenching of fluorescence

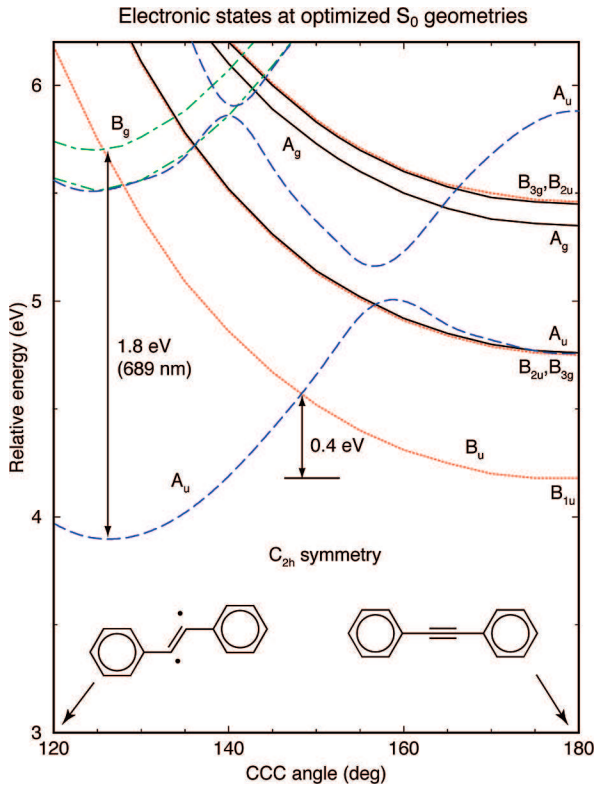

FIGURE 2. TD/BLYP/6-31G* electronic states of DPA, at optimized S_0 geometry. The energies are calculated at the optimized ground-state geometries for a given CCC angle. Vertical arrow indicates A_u ($\pi\sigma^*$) → B_g ($\pi\sigma^*$) transition in the bent molecule. The CC stretching frequency of $\pi\sigma^*$ state is 1547 cm^{-1}. Reprinted with permission from ref 3.

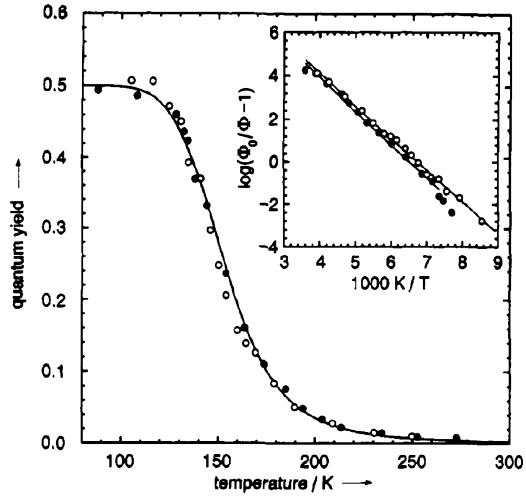

FIGURE 3. Temperature dependence of the fluorescence quantum yield of DPA in 3-methylpentane (○) and EPA (●). EPA stands for diethyl ether−isopentane−ethanol mixture (volume ratio 5:2:5). The inset shows the same data as a linearized Arrhenius plot. Reprinted with permission from ref 4. Copyright 1993 American Chemical Society.

occurs, in solution, is similar to the ~500 cm^{-1} onset of the fluorescence break-off in the supersonic free jet (Figure 1).

The calculations further predict that the $\pi\sigma^*$ state of bent geometry can be identified by the greatly reduced frequency (1547 cm^{-1}) of acetylenic C—C stretch (resulting from the decrease in bond order from three to two)[3] and a strong $\pi\sigma^*$ ← $\pi\sigma^*$ absorption that is expected at about 700 nm.[3] These predictions are borne out by the observation of the temperature- and viscosity-dependent transient absorption at about 700 nm,[5] Figure 4a, and the greatly reduced C—C stretching frequency (1570 cm^{-1}) of the "lowest excited single state", which has been observed in the time-resolved CARS (coherent anti-Stokes Raman spectroscopy).[6]

Consistent with the formation of the $\pi\sigma^*$ state from the initially prepared $\pi\pi^*$ (B_{1u}) state, the decay time of $\pi\pi^*$-state transient at about 500 nm, which is the same as the fluorescence decay time, agrees with the rise time of the $\pi\sigma^*$-state absorption at about 700 nm.[5] Interestingly, the calculations also show that the attachment of an electron-withdrawing group (such as −CN and $-COOCH_3$) to DPA increases the energy of the $\pi\sigma^*$ state and moves the $\pi\pi^*/\pi\sigma^*$ intersection far away from Franck−Condon region (viz., $\theta \approx 180°$) of the initially prepared $\pi\pi^*$ state,[7] Figure 5, such that the lowest excited (S_1) state is $\pi\pi^*$ in *p*-CH_3COO−DPA and *p*-CN−DPA. The $\pi\pi^* \rightarrow \pi\sigma^*$ state switch is therefore not expected to occur in DPA with an electron-withdrawing substituent.[7] Consistent with these predictions, *p*-CH_3COO−DPA and *p*-CN−DPA do not exhibit 700 nm transient, characteristic of the $\pi\sigma^*$ state,[5] Figure 4b, and the fluorescence lifetime (and quantum yield) of these molecules do not exhibit temperature dependence.[5] Conversely, the electron-donating group enhances the state switch from the initially excited $\pi\pi^*$ state to the $\pi\sigma^*$ state, as demonstrated in Figure 4c.[7]

It may be useful here to note that benzene[8,9] and azabenzenes[10] also exhibit a significant loss of the gas-phase fluorescence at higher excitation energies (~3000 cm^{-1} above the S_1 origin for benzene and ~2000 cm^{-1} in pyridine). This loss of fluorescence is known to be due to the greatly enhanced $S_1 \rightarrow S_0$ internal conversion,[11] but the question of whether the nonradiative passage from S_1 to S_0 is a direct two-state process or an internal conversion mediated by a photochemical intermediate (prefulvene)[12] is not settled.[13]

Extension of the computational study to di-2-thienylacetylene (DTA) and di-2-furylacetylene (DFA) indicates that the dark $\pi\sigma^*$ state is either very slightly above (DTA) or slightly below (DFA) the lowest-energy $^1\pi\pi^*$ state at the linear geometry,[14] Figure 6. The state crossing from the $^1\pi\pi^*$ to the $^1\pi\sigma^*$ state is therefore expected to involve little (if any) energy barrier. Consistent with this prediction, DTA and DFA do not exhibit fluorescence in solution at room temperature.

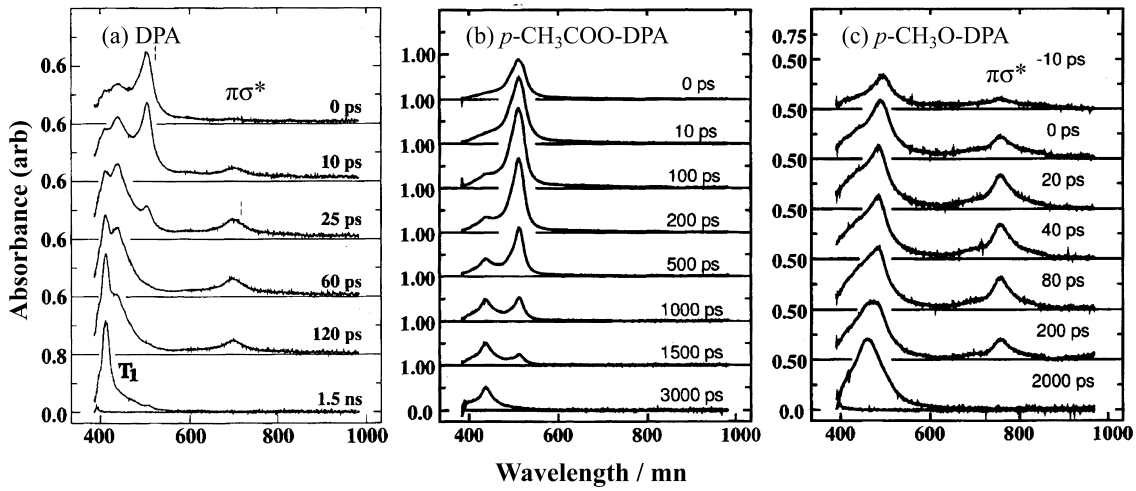

FIGURE 4. Time-resolved transient absorption spectra of DPA, CH_3COO−DPA, and CH_3O−DPA in *n*-hexane, as a function of pump−probe delay time. The feature at about 700 nm is due to the absorption from $\pi\sigma^*$ state. Adapted with permission from ref 5.

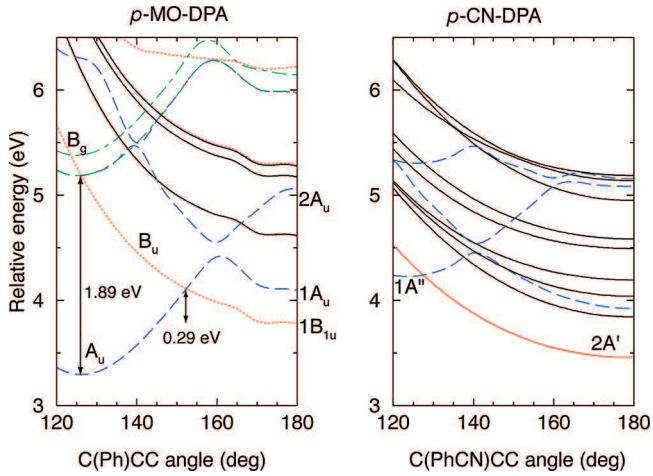

FIGURE 5. TD/BP86/6-31G* energies of excited electronic states for *p*-MO−DPA and *p*-CN−DPA. Reprinted with permission from ref 7.

4-(Dimethylamino)benzethyne. The presence of a low-lying $\pi\sigma^*$ state is also very evident in phenylacetylenes containing electron-donating substituents, for example, 4-(dimethylamino)benzethyne (DMABE).[15] The $\pi\sigma^*$ state of such molecule is highly polar relative to the lowest-energy $\pi\pi^*$ (L_b) state, thus allowing its identification via solvent-polarity dependence of excited-state absorptions.[15] Figure 7a presents the transient absorption spectra of DMABE in acetonitrile and *n*-hexane at room temperature, recorded with pump−probe delay of 0.6 ps, following 305 nm femtosecond excitation of the molecule into the L_a ($\pi\pi^*$) state.[15] The spectra are composed of two major features with intensity maxima at about 700 and 520 nm. Comparison of the observed band positions with the TDDFT/BP86/cc-pVDZ vertical excitation wavelengths, Figure 7c, allows the assignment of the 700 nm transient to the $\pi\sigma^*$-state absorption and the 520 nm transient to the LE (L_b)-state absorption, as listed in Table 1.[15] These assignments are supported by the blue shift of the longer-wavelength transient in going from the *n*-hexane (720 nm) to acetonitrile (680 nm) and by the differing decay times of the 700 and 520 nm transients, Figure 7b. The bifurcation of the initially excited L_a ($\pi\pi^*$) into the $\pi\sigma^*$ state and the L_b (LE) state, as probed by transient absorption, is strongly influenced by solvent polarity, with polar environment favoring the $L_a \rightarrow \pi\sigma^*$ decay channel over the competing $L_a \rightarrow L_b$ decay channel.[15] This accounts for the observation that the 700 nm $\pi\sigma^*$-state transient is much more intense than the 520 nm L_b-state absorption in acetonitrile, whereas it is less intense in *n*-hexane. The nanosecond radiationless decay of the L_b (LE) state to the dark $\pi\sigma^*$ state is also strongly enhanced in a polar environment, leading to a dramatic quenching of the fluorescence in solvents of high polarity.[16,17]

Aromatic Nitriles: 4-(Dimethylamino) benzonitrile in Particular

4-(Dimethylamino)benzonitrile, DMABN, is isoelectronic with DMABE, and hence the electronic structures and electronic spectra of the two compounds are expected to bear very close resemblance.[15] Consistent with these expectations, both the steady-state absorption and fluorescence spectra of the two compounds are very similar in nonpolar solvents, as illustrated in Figure 8 (right panels). In polar solvents, on the other hand, there is a major difference in the fluorescence spectra of the two compounds, Figure 8 (left). Thus, unlike DMABE that exhibits single fluorescence from the L_b ($\pi\pi^*$) state, DMABN exhibits dual fluorescence in polar solvents:[18] the normal fluorescence from the L_b state, referred to as the locally excited (LE) emission, and the greatly red-shifted fluorescence from the intramolecular charge transfer state.[19]

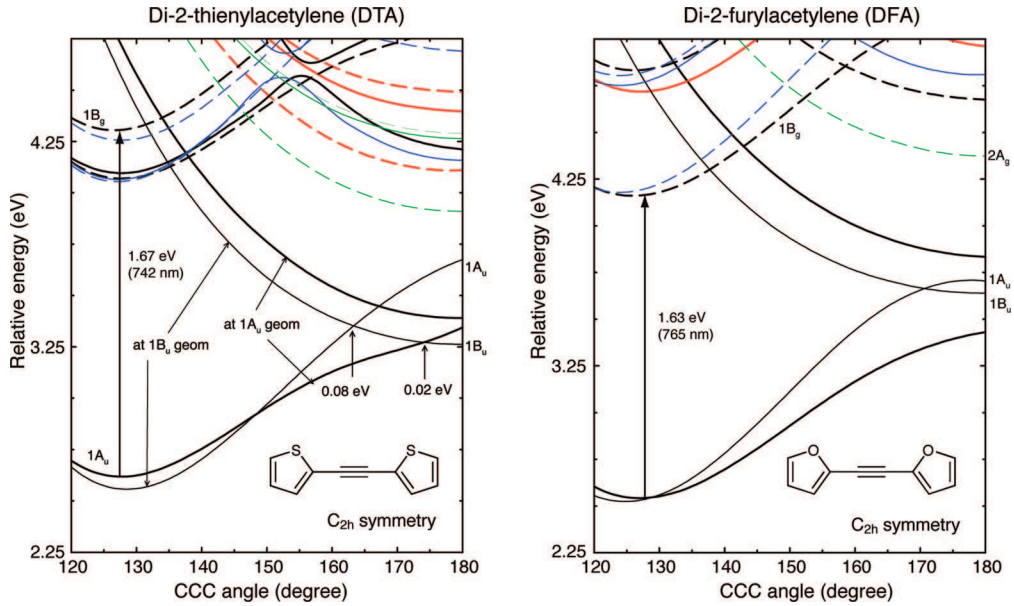

FIGURE 6. TD/BP86/cc-pVDZ energies at CIS geometries of di-2-thienylacetylene (DTA) and di-2-furylacetylene (DFA).

The intramolecular charge transfer (ICT) in DMABN and related dialkylaminobenzonitriles in polar solvents, leading to the appearance of the dual fluorescence, has been a topic of very extensive experimental and computational studies for several decades.[20] The two fundamental issues associated with the dual emissions of dialkylaminobenzonitriles are the geometrical structure of the emitting ICT state, and the reaction pathway that connects the initially excited L_a-like $\pi\pi^*$ state to the ICT state. The first of these has largely centered on the question of whether the ICT state of DMABN (which arises from the transfer of an electron from the dimethylamino group to the benzonitrile moiety) has a twisted amino group (TICT) or a planar amino group (PICT) relative to the plane of the phenyl ring. Experimental support for the TICT model, which is due to Grabowski and co-workers, comes from the observation that aminobenzonitriles with pretwisted amino group (e.g., 3,5-dimethyl-4-DMABN) exhibit only the ICT fluorescence.[20,21] On the other hand, the observation of dual fluorescence from the "planar" 1-*tert*-butyl-6-cyano-1,2,3,4-tetrahydroquinoline (NTC6) provides support for the PICT model of Zachariasse et al.[22] A majority, if not all, of the theoretical studies indicate the amino group twist as the reaction coordinate for the L_a ($\pi\pi^*$) → ICT transition.[23] Moreover, NTC6 and related alicyclic analogs of DMABN have been shown to be flexible enough to yield TICT geometry upon electronic excitation.[24,25]

The second issue has to do with the reaction pathway connecting the initially excited L_a state to the ICT state. From the very extensive time-resolved emission studies of DMABN and related aminobenzonitriles, which yield a rise time of the ICT fluorescence that is "identical" to the initial decay of the LE fluorescence, it has long been assumed that the ICT state is formed directly from the LE state (following the L_a → LE internal conversion).[26] The TDDFT excited-state calculations of DMABN, Figure 9, however, indicate the presence of a $\pi\sigma^*_{CN}$ state, lying below the LE ($\pi\pi^*$) state, which may be involved in the ICT reaction.[27,28] The existence of a low-lying $\pi\sigma^*$ state is supported by the LE fluorescence break-off in supersonic free jet[29] and by the strong thermal quenching of the LE fluorescence of DMABN in nonpolar solvents[30] where no ICT reaction occurs, which are very similar to the observations in diphenylacetylene.

Figure 10a,b shows the femtosecond time-resolved transient absorption spectra of DMABN in acetonitrile, measured with a series of pump−probe delays (−1 to 25 ps).[31] The 680 and 520 nm transients of DMABN can be assigned to the $\pi\sigma^*$-state and $\pi\pi^*$ (L_b)-state absorptions, respectively, on the basis of their very close resemblance to the computed vertical transition energies,[28] Table 2. The transients at 420 and 320 nm, which appear only in polar solvents, are very similar[32] to the absorption spectrum of the benzonitrile radical anion[33] in both peak positions and relative intensities,[34] as shown in Figure 10a. Moreover the time-resolved Raman spectra of the ICT state, obtained by using a probe (Raman-inducing) wavelength of 400 nm, exhibit several characteristic modes that are very similar to the modes observed for the benzonitrile radical anion.[35] These results strongly indicate that the ICT transient observed in the time-resolved absorption experiment is the zwitterionic TICT state, in which 90° twisted geometry of the

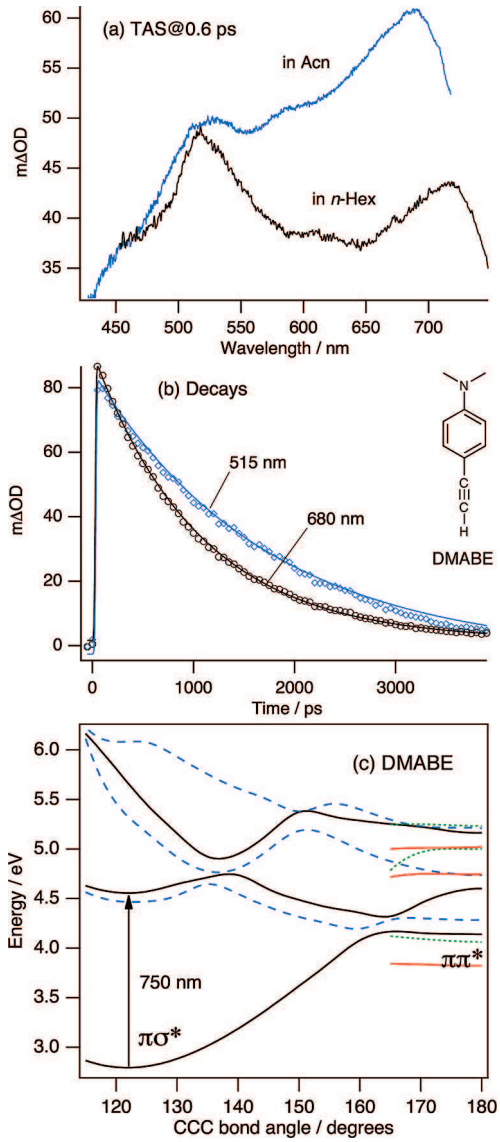

FIGURE 7. (a) The excited-state absorption spectra of DMABE in acetonitrile (Acn) and *n*-hexane (Hex) at room temperature following a 305 nm excitation, (b) the temporal profiles of 680 and 520 nm transient absorptions in Acn, and (c) TDDFT energy of low-lying $\pi\pi^*$ and $\pi\sigma^*$ singlet states of DMABE as a function of $C_{Ph}CC$ angle, as calculated using the TD/BP86/cc-pVDZ level of theory. The solid curves are for the optimized CIS/cc-pVDZ geometries of the $\pi\sigma^*$ state, whereas the dotted curves are for the corresponding optimized $\pi\pi^*$ state. The vertical arrow denotes the highly allowed $\pi\sigma^* \leftarrow \pi\sigma^*$ transition. Reprinted with permission from refs 15 and 31.

amino group with respect to the benzene ring leads to electronic decoupling of the dimethylamino and benzonitrile moieties.

The picosecond rise time (4.3 ps) of the TICT-state absorption at 420 nm is identical to the decay time of the $\pi\sigma^*$-state absorption at 680 nm for DMABN in acetonitrile,[31,36] Figure 10d,e, thus establishing the precursor−successor relationship between the two states. The same conclusion has been

TABLE 1. Comparison of TDDFT/BP86/cc-pVDZ Vertical Excitation Wavelengths (λ) and Oscillator Strengths (f) of the $\pi\sigma^*$- and LE-State Absorptions in DMABE with Experimental Values

transition	calcd λ (nm)[a]	f	exptl λ (nm)[b]
$\pi\sigma^* \leftarrow \pi\sigma^*$	750	0.6[c]	715
$\pi\pi^* \leftarrow \pi\pi^*$ (LE)	528	0.15[c]	520

[a] Only transitions with f greater than 0.06 in the 430−800 nm range are listed. [b] In *n*-hexane. [c] The average of coordinate and velocity gauges.

reached from the temporal measurements of the subpicosecond $\pi\sigma^*$ and TICT transients of 4-(diisopropylamino)benzonitrile, DIABN, in acetonitrile at room temperature.[31,36]

The $\pi\sigma^*$-mediated ICT reaction model is further supported by the absence of the ICT fluorescence or the TICT transient in acetonitrile solution of DMABE. Table 3 compares the adiabatic excitation energies of the L_a ($\pi\pi^*$), LE ($\pi\pi^*$), $\pi\sigma^*$, and TICT states of DMABE and DMABN, calculated by the TDDFT methods.[15] It should be noted that the TICT state of DMABE lies above the $\pi\sigma^*$ state, whereas the opposite is the case in DMABN. The absence of an ICT reaction in DMABE can therefore be explained within the context of the $\pi\sigma^*$-mediated ICT model.

The picture emerging from the time-resolved spectroscopy of DMABN and DIABN is that the initially excited L_a ($\pi\pi^*$) state bifurcates into the LE and $\pi\sigma^*$ state in less than 200 fs, the shortest time delay in the transient absorption experiments. In polar solvent, the dark $\pi\sigma^*$ state of DMABN produces the TICT state via the charge-shift reaction, as we have previously proposed, Figure 11 (left). The identity of the decay time of the $\pi\sigma^*$ transient at about 700 nm and the formation time of the TICT transient at about 420 nm in DMABN and DIABN provides compelling evidence in support of the $\pi\sigma^*$-mediated TICT mechanism. The primary energetic requirement for the formation of the TICT state is the presence of the $\pi\sigma^*$ state that lies between the initially excited $\pi\pi^*$ state and the ICT state, Figure 11 (right). This condition is apparently met in DMABN and DIABN, which exhibit TICT reaction in polar solvents, but not for 2-DMABN, 3-DMABN, and ABN in any solvent or for DMABN in nonpolar solvents.[31]

The $\pi\sigma^*$-mediated formation of the TICT state is supported by a recent CASPT2/CASSCF calculation of Coto et al.[37] on DMABN in acetonitrile, which demonstrates that the $\pi\sigma^*$ state lies in between the initially excited $\pi\pi^*$ state (L_a) and the TICT state. In the minimum of the $\pi\sigma^*$ state, the C−C bond in the C_{Ph}−CN elongates and the CN group is bent. It is the effect of polar solvent, which lowers the energy of the highly polar $\pi\sigma^*$ state with a large dipole moment.

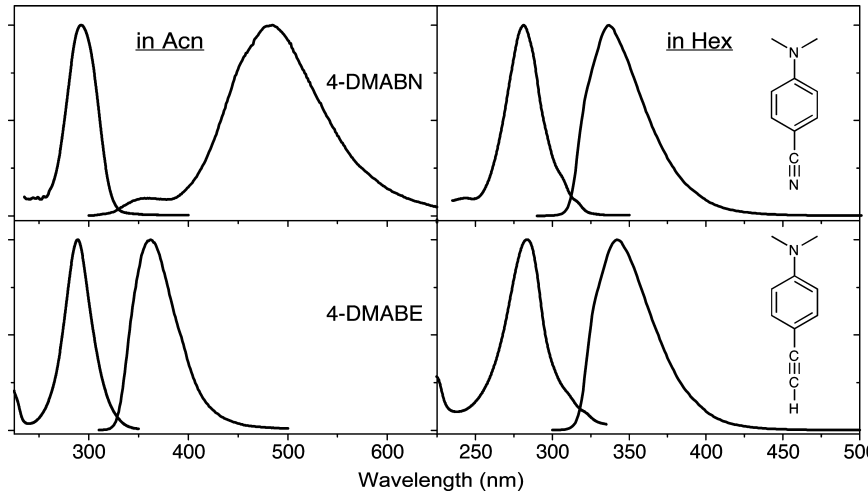

FIGURE 8. Comparison of the steady-state absorption and emission spectra of DMABN and DMABE in acetonitorile and *n*-hexane solvents.

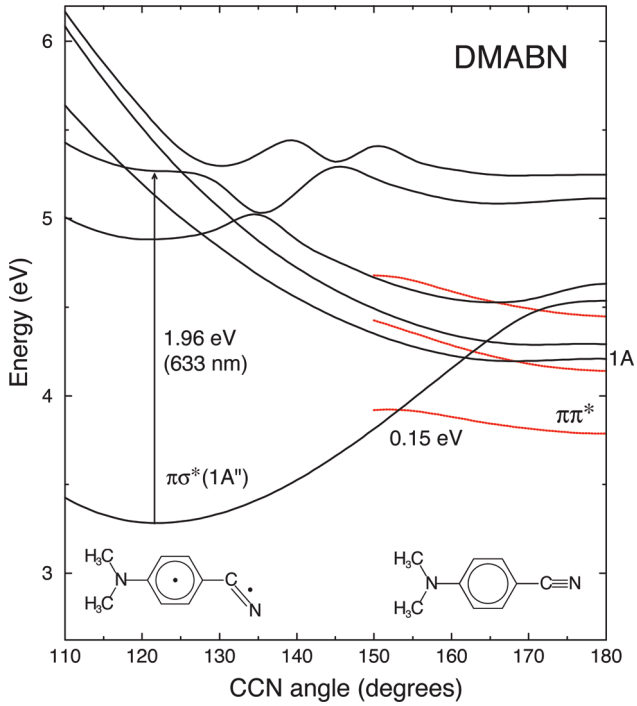

FIGURE 9. TDDFT energies of low-lying excited singlet states of DMABN as a function of $C_{Ph}CN$ angle, as calculated using the TD/BP86/6-311++G** level of theory. Reprinted with permission from ref 27.

Nature of the ICT State

The time-resolved fluorescence measurements, using the time-correlated single-photon counting (TCSPC) method, which indicate that the fluorescent ICT state of DMABN is formed from the LE state,[26] are at odds with the time-resolved transient absorption measurements, which demonstrate that the TICT state of DMABN is formed from the $\pi\sigma^*$ state.

Given that the TCSPC method has a typical instrument response function (≥30 ps) that is slow compared with the time scale of the ICT reaction in DMABN (~4 ps in acetonitrile) or DIABN (≤1 ps in acetonitrile), it is essential to carry out fluorescence upconversion experiments on DMABN and DIABN, using an experimental setup that has an apparatus function of approximately 350 fs (fwhm). The results of these measurements[36] have shown that the rise time (3.0 ps) of the ICT fluorescence of DMABN at 550 nm is identical to the decay time (3.0 ps) of the LE fluorescence at 350 nm, thus confirming the precursor−successor relationship between the LE and ICT states.

The possibility, therefore, exists that the fluorescent ICT state differs from the TICT state observed in transient absorption, because the extremely small oscillator strength (f = 0.000)[38] of the TICT state should render the state essentially nonfluorescent. To be more specific, the radiative lifetime (τ_r) of the TICT state can be estimated from ($\tau = 1.5/(f\bar{\nu}^2)$, where f is the oscillator strength of the electronic transition and $\bar{\nu}$ is the mean frequency (in cm^{-1}) of the ICT fluorescence. Using $f = 1 \times 10^{-4}$ from a TDDFT BP86/cc-pVDZ calculation,[39] one obtains $\tau_r \cong 38\ \mu s$ for the fluorescence from the TICT state. This translates to the ICT fluorescence quantum yield of $\sim 8 \times 10^{-5}$, when combined with the measured fluorescence lifetime of 2.9 ns. This is more than 2 orders of magnitude smaller than the measured quantum yield of the ICT fluorescence (0.030),[26] suggesting that the CT state observed in the fluorescence is not the TICT state.

Consistent with this supposition, the rise time as well as the decay time of the ICT-state absorption differs from the corresponding time scales of the ICT fluorescence in DMABN. Thus, the rise time (~4.3 ps) of the TICT-state transient absorption at 420 nm is significantly longer than that (3.0 ps) of the ICT emission at 550 nm, measured by fluorescence upconversion.[36] The differing rise times indicate that the fluorescent ICT state is not the same as the TICT

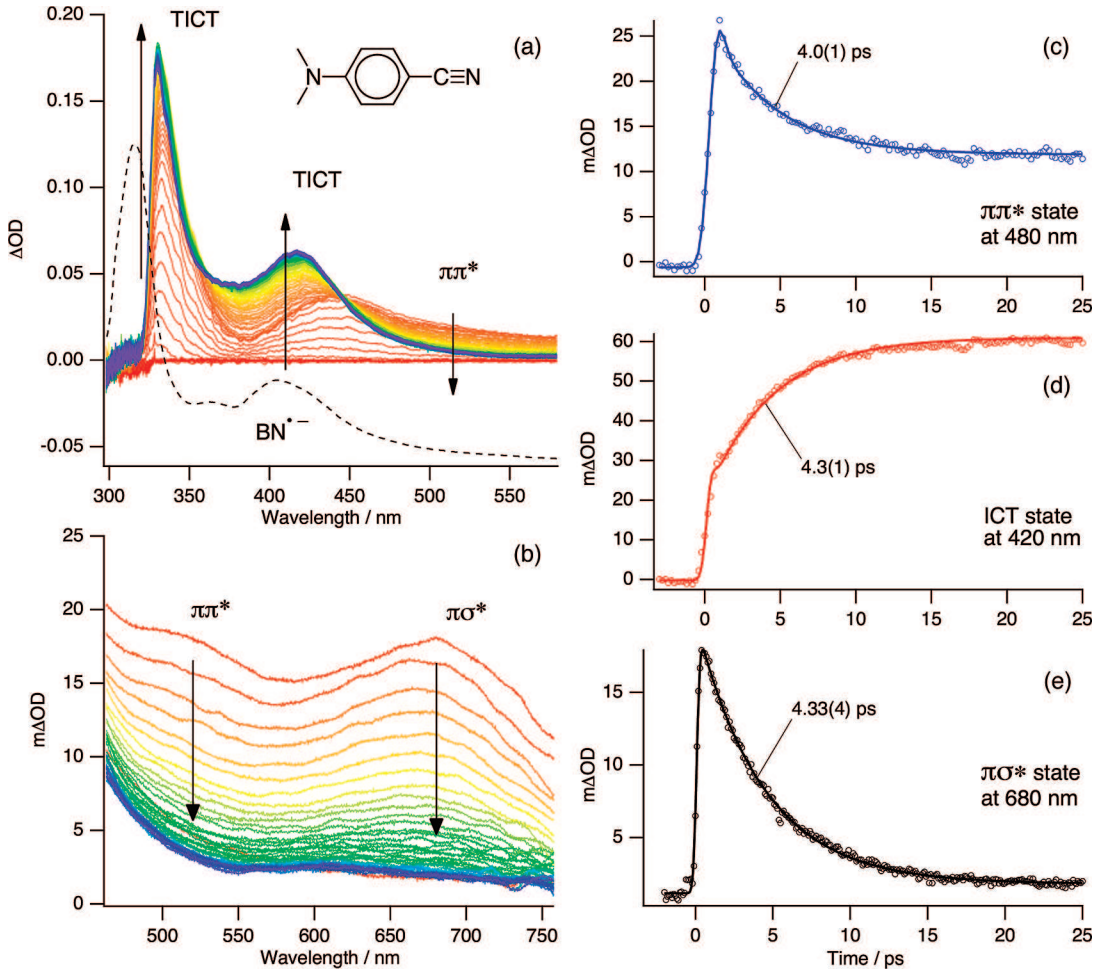

FIGURE 10. Femtosecond time-resolved transient absorption spectra of DMABN in acetonitrile at room temperature (λ_{exc} = 267 nm) for (a) shorter and (b) longer wavelength ranges with the pump−probe delays (−1 to 25 ps). Arrows indicate the time evolution of the spectra, and assignments for the transients are also shown. The dashed curve is the ground-state absorption spectrum of benzonitrile radical anion ($BN^{\bullet-}$) adapted from ref 33. Temporal decay profiles of (c) the 480 nm transient (LE/$\pi\pi^*$ state), (d) the 420 nm TICT transient, and (e) the 680 nm for the $\pi\sigma^*$-state absorption of DMABN in acetonitrile at the excitation of 267 nm, which were extracted by band integration from the time-resolved spectra a and b. The values in parentheses of the rise or decay constant indicate a standard deviation (1σ) to the final digit. Adapted with permission from ref 36.

TABLE 2. Comparison of TDDFT/BP86/cc-pVDZ Vertical Excitation Wavelengths (λ) and Oscillator Strengths (f) of the $\pi\sigma^*$- and $\pi\pi^*$ LE-State Absorptions in DMABN with Experimental Values

transition	calcd λ (nm)[a]	f[b]	exptl λ (nm)[c]
$\pi\sigma^* \leftarrow \pi\sigma^*$	640	0.55 (0.50)	700
$\pi\pi^* \leftarrow \pi\pi^*$	524	0.07 (0.08)[c]	525
$\pi\pi^* \leftarrow \pi\pi^*$	423	0.08 (0.14)	450

[a] Only transitions greater than 0.07 are listed. [b] The number in parentheses represents the transition moment. [c] From ref 31.

TABLE 3. Comparison of TDDFT/BP86/cc-pVDZ Adiabatic Excitation Energies (in eV) of 4-DMABE and 4-DMABN

state	DMABE	DMABN[a]
L_a	4.38	4.50
LE	4.16	4.28
$\pi\sigma^*$	3.43	4.20
TICT	4.14	3.46

[a] From ref 15.

state observed in the transient absorption. Similarly, the nanosecond decay time (~2.9 ns) of the ICT fluorescence is also different from the decay time (~4.8 ns) of the TICT-state absorption for DMABN in acetonitrile.[36] Moreover, the decay time of the TICT-state absorption at 320 nm is substantially longer than the decay time of the ICT emission.[40] This again indicates that the ICT state observed in fluorescence is different from the TICT state observed in transient absorption.

The proposal that the fluorescent ICT state is not the same as the TICT state (observed in the transient absorption experiment) is also supported by the observation that DIABN, which exhibits ICT fluorescence (as well as the LE fluorescence) even

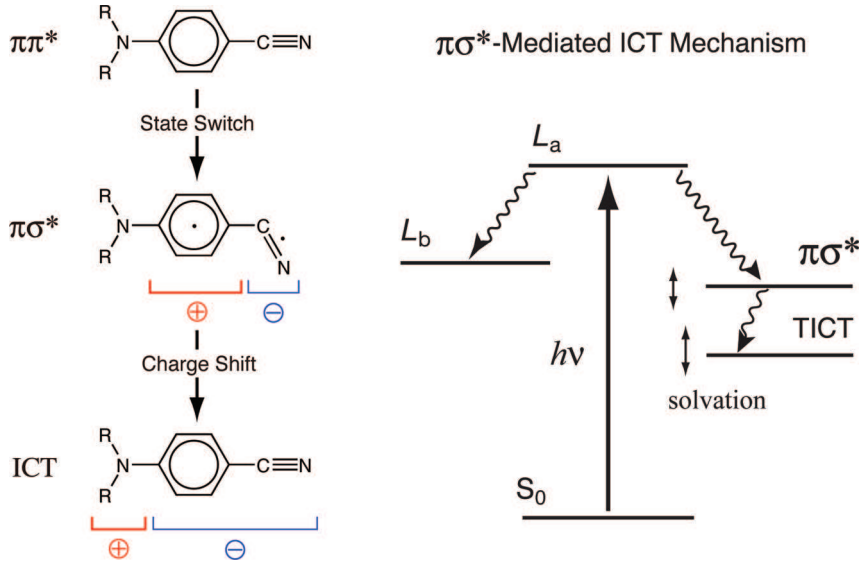

FIGURE 11. Schematic mechanism for dialkylaminobenzonitriles (left panel) and energy level diagram for the $\pi\sigma^*$-state-mediated intramolecular charge transfer. Adapted with permission from ref 31 (right).

in nonpolar solvents, does not display the 410 nm transient absorption, characteristic of the zwitterionic TICT state in *n*-hexane.[31]

Similar discrepancies between the time constants of the TICT-state absorption and the ICT fluorescence exist for DMABN in ethanol. Thus, the 9.9 ps rise time and the 3.3 ns decay time of the 420 nm TICT-state absorption are significantly greater than the 6.0 ps rise time and 2.3 ns decay time of the ICT fluorescence at room temperature.[36]

Fluorinated Benzenes

Polyfluorinated benzenes are the third class of molecules that possess a bound S_1 ($\pi\sigma^*$) state.[41] From the early spectroscopic[42−44] and photophysical[45,46] studies of the fluorinated benzenes, it is known that the spectral features of the absorption and emission, as well as the lifetime of the fluorescence, depend strongly on the number of fluorinated atoms. Thus, $C_6H_{6-n}F_n$ with four or less F atoms, $n = 1-4$, exhibit structured $S_1 \leftarrow S_0$ absorption and fluorescence spectra, strong fluorescence, and nanosecond fluorescence lifetimes, whereas those with five or six F atoms display structureless absorption/excitation spectra,[42−44] very weak fluorescence,[45,46] and biexponential fluorescence decays with picosecond and nanosecond lifetimes.[47] These differences suggest that the nature of the lowest excited singlet state may be different for the two classes of the compounds, despite the previous $\pi\pi^*$ assignment of S_1 for all fluorinated benzenes.[42,44] More specifically, it is possible that the $^1\pi\sigma^*$ state, which is formed by the promotion of an electron from the ring-centered π orbital to the σ^* orbital, localized on the C−F bond, could be the emitting state in molecules with high degrees of fluorination (i.e., $n = 5, 6$).

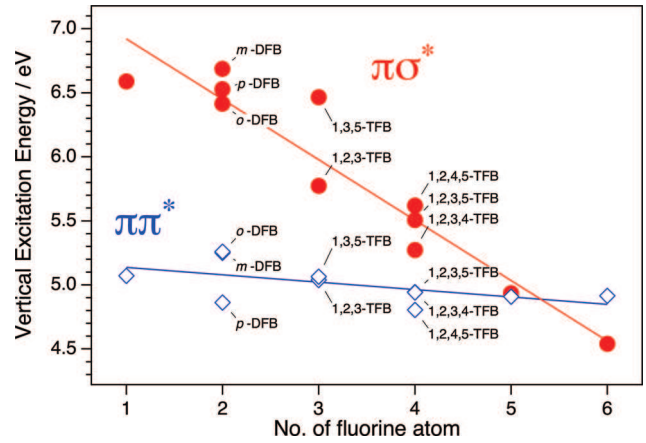

FIGURE 12. A plot of the TDDFT vertical excitation energies of the lowest-energy $\pi\pi^*$ state and the lowest-energy $\pi\sigma^*$ state as a function of the number of fluorine atoms. Reprinted with permission from ref 41.

Figure 12 presents the TDDFT vertical excitation energies for the lowest-energy $^1\pi\pi^*$ and $^1\pi\sigma^*$ states at optimized ground-state geometry.[41] The results show that while the vertical excitation energy of the $\pi\pi^*$ state decreases slowly with increasing number of fluorine atoms, the vertical excitation energy of the $\pi\sigma^*$ state decreases rather rapidly with increasing degree of fluorination. As a consequence, the $\pi\sigma^*$ state with an elongated C−F bond is expected to lie very close to or lower than the first $\pi\pi^*$ state in pentafluorobenzene (PFB) and below the $^1\pi\pi^*$ state in hexafluorobenzene (HFB). The calculation also indicates that the $\pi\sigma^*$ state is highly polar and has equilibrium geometry that is characterized by out-of-plane deformed C−F bonds. Moreover, the electronic transition from

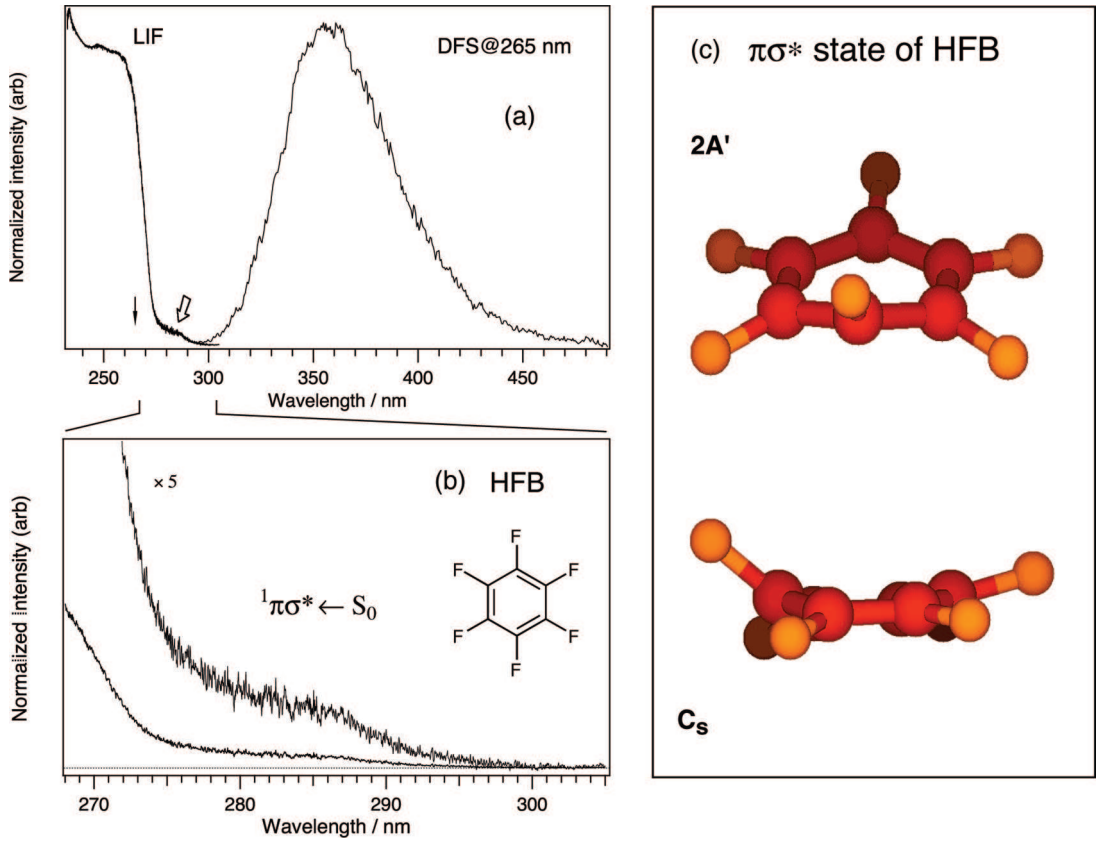

FIGURE 13. (a) Fluorescence excitation and dispersed fluorescence spectra (DFS) of HFB in supersonic free jet. The open arrows denote the feature assigned to the $^1\pi\sigma^* \leftarrow S_0$ absorption, whereas the sold arrows indicate the excitation wavelength for the dispersed emissions. (b) The expanded features of the LIF spectrum in panel a. (c) Two views of the optimized geometries of the lowest-energy $\pi\sigma^*$ state of HFB. Reprinted with permission from ref 41.

the planar ground state to the nonplanar $^1\pi\sigma^*$ state is essentially forbidden in PFB and HFB. Thus, following the optical excitation to the Franck−Condon $^1\pi\pi^*$ state, electronic charge distribution shifts from the benzene ring to the C−F bond through $\pi^* \rightarrow \sigma^*$ electron transfer. The $\pi\sigma^*$ state of the fluorinated benzenes is therefore a charge-transfer state as well as a biradical state.

The assignment of S_1 to the $\pi\sigma^*$ state for both HFB and PFB is supported by the fluorescence excitation and dispersed fluorescence spectra of HFB in supersonic free jet,[41] shown in Figure 13a. Excitation to the first $\pi\pi^*$ state at $\lambda = 265$ nm leads to a strongly red-shifted, broad, structureless emission with intensity maximum at $\lambda = 360$ nm. The large Stokes shift, the absence of spectral overlap between the fluorescence and the lowest-energy $\pi\pi^* \leftarrow S_0$ absorption bands, and the significantly larger spectral width of the emission compared with the absorption band clearly point out that the fluorescence originates from a state at lower energy than the lowest energy $\pi\pi^*$state. With the detection of a very weak absorption band to the red of the origin of the first $\pi\pi^*$ state in the LIF excitation spectrum, Figure 13b, it is possible to identify the S_1 ($\pi\sigma^*$) state as the fluorescent state.[41] The small fluorescence quantum yield ($\Phi_F = 0.05$) is consistent with the very small radiative transition probability of the $\pi\sigma^*$ state.

Remarkably, excitation of HFB to the S_2 ($\pi\pi^*$) state by femtosecond laser pulses leads to the appearance of large-amplitude oscillations (of frequency ~100 cm^{-1}) in the femtosecond transient absorption in solution,[48] as well as in the femtosecond multiphoton ionization in a supersonic free jet.[49] The most surprising aspect of the quantum coherence in jet-cooled HFB is that the oscillatory behavior is preserved for the entire range of the pump laser wavelength (265−217 nm) used to excite the S_2 ($\pi\pi^*$) and S_3 ($\pi\pi^*$) states. Although the question of whether the oscillations originate from the electronic coherence[48] (between the optically excited $\pi\pi^*$ state and the $\pi\sigma^*$ state) or from the vibrational coherence[49] (involving a low-frequency out-of-plane mode in the $\pi\sigma^*$ state) is unclear, there is little doubt that coupling (via an out-of-plane vibrational mode) between the close-lying first $\pi\pi^*$ state and a lower-lying $\pi\sigma^*$ state is the reason for these highly interesting observations.

Another class of halogenated benzenes with a bound $\pi\sigma^*$ state with elongated C−X (X = halogen) bond are chlorobenzenes. In rigid glass at low temperature, chlorobenzenes and *p*-dichlorobenzene exhibit dual phosphorescence, which is believed to originate from two low-lying triplet states. Takemura et al.[50] assigned the longer-wavelength, longer-lived emission to the lowest triplet (T_1) state of $\pi\sigma^*$ character. These assignments have been supported by HF/3-21G calculations of Nagaoka et al.,[51] which indicate the presence of a $^3\pi\sigma^*$ state with a long C−Cl bond slightly above the T_1 ($\pi\pi^*$) state. Since the $^1\pi\sigma^*-^3\pi\sigma^*$ electronic gap is expected to be much smaller than the $^1\pi\pi^*-^3\pi\pi^*$ energy gap, it is possible that the lowest-energy $^1\pi\sigma^*$ state is the S_1 state of the molecule in some of the polychlorinated benzenes. Consistent with such a supposition, 1,4-dichlorobenzene and hexachlorobenzenes are nonfluorescent compounds.

Unlike the fluorinated and chlorinated benzenes, the $\pi\sigma^*$ state of bromobenzenes is repulsive along the C−Br stretching coordinate.[52] In several of gaseous bromoflorobenzenes, the main dissociation channel following 270 nm excitation is a predissociation involving the bound S_1 ($\pi\pi^*$) state and a repulsive $^3\pi\sigma^*$ state, giving rise to the dissociation rates of 20−40 ps.[52] In di- and pentafluorobromobenzenes, where a repulsive $^1\pi\sigma^*$ state lies lower in energy, a direct excitation to the state leads to a subpicosecond (<300 fs) dissociation rate.[52]

Concluding Remarks

In this Account, we have presented the experimental and theoretical work concerning the excited-state dynamics of molecules that possess the lowest excited singlet state of $\pi\sigma^*$ configuration, which arises from the promotion of an electron from the π orbital of the phenyl ring to the σ^* orbital localized on the −C≡X (X = CH and N) group or on the C−F group. Because of the greatly different equilibrium geometry of the $\pi\sigma^*$ states, the S_1 ($\pi\sigma^*$) state crosses the initially excited $\pi\pi^*$ state along the stretching of the C−F bond and bending of the C≡X (X = CH or N) group. These crossings not only greatly affect electronic relaxation but also induce $\pi\sigma^*$-mediated intramolecular charge transfer in dialkylaminobenzonitriles.

We are grateful to the U.S. Department of Energy and Ohio Supercomputer Center for the financial support, and to Drs. Ricardo Campos Ramos and Jae-Kwang Lee for their contributions to the work described in this Account.

BIOGRAPHICAL INFORMATION

Marek Z. Zgierski received his Ph.D. in 1971 and D.Sc in 1976 from the Jagiellonian University in Kracow, Poland. In 1977, he joined National Research Council of Canada in Ottawa, where he is a Senior Research Officer. His primary scientific interests are radiationless transitions and manifestation of vibronic coupling in various branches of spectroscopy of polyatomic molecules.

Takashige Fujiwara is a senior research associate at The University of Akron. He received his M.S. (1993) and Ph.D. (2000) from Kyoto University, Japan. His primary research interests are in molecular excited-state dynamics on the basis of the ultrafast and the high-resolution laser spectroscopies.

Edward C. Lim received his Ph.D. in 1959 from Oklahoma State University. He was on the faculty at Loyola University before moving to Wayne State University (1969−1989). He joined the University of Akron as Goodyear Professor in 1989. His research interests are in electronic spectroscopy and molecular photophysics of organic molecules.

FOOTNOTES

*Corresponding author. E-mail: elim@uakron.edu.

§Holder of Goodyear Chair in Chemistry.

REFERENCES

1 Klessinger, M.; Michl, J. *Excited States and Photochemistry of Organic Molecules*; VCH: New York, 1995.

2 Okuyama, K.; Hasegawa, T.; Ito, M.; Mikami, N. Electronic Spectra of Tolan in a Supersonic Free Jet: Large-Amplitude Torsional Motion. *J. Phys. Chem.* **1984**, *88*, 1711–1716.

3 Zgierski, M. Z.; Lim, E. C. Nature of the 'Dark' State in Diphenylacetylene and Related Molecules: State Switch from the Linear $\pi\pi^*$ State to the Bent $\pi\sigma^*$ State. *Chem. Phys. Lett.* **2004**, *387*, 352–355.

4 Ferrante, C.; Kensy, U.; Dick, B. Does Diphenylacetylene (Tolan) Fluoresce from Its Second Excited Singlet State? Semiempirical MO Calculations and Fluorescence Quantum Yield Measurements. *J. Phys. Chem.* **1993**, *97*, 13457–13463.

5 Hirata, Y. Photophysical and Photochemical Primary Processes of Diphenylacetylene Derivatives and Related Compounds in Liquid Phase. *Bull. Chem. Soc. Jpn.* **1999**, *72*, 1647–1664, and references therein.

6 Ishibashi, T.; Hamaguchi, H. Structure and Dynamics of S_2 and S_1 Diphenylacetylene in Solution Studied by Picosecond Time-Resolved CARS Spectroscopy. *J. Phys. Chem. A* **1998**, *102*, 2263–2269.

7 Zgierski, M. Z.; Lim, E. C. On the Mechanism of Intramolecular Charge Transfer in para-Disubstituted Diphenylacetylenes Containing Electron-Donating and Electron-Accepting Groups: Role of $\pi\sigma^*$ State in Electron-Transfer Dynamics. *Chem. Phys. Lett.* **2004**, *393*, 143–149.

8 Parmenter, C. S.; Schyler, M. W. Single Vibronic Level Fluorescence. III. Fluorescence Yields from Three Vibronic Levels in the $1B_{2u}$ State of Benzene. *Chem. Phys. Lett.* **1970**, *6*, 339–341.

9 Parmenter, C. S. Radiative and Nonradiative Processes in Benzene. *Adv. Chem. Phys.* **1972**, *22*, 365–421.

10 Yamazaki, I.; Murao, T.; Yamanaka, T.; Yoshihara, K. Intramolecular Electronic Relaxation and Photoisomerization Processes in the Isolated Azabenzene Molecules Pyridine, Pyrazine, and Pyrimidine. *Faraday Discuss. Chem. Soc.* **1983**, 395–405.

11 Nakashima, N.; Yoshihara, K. Laser Photolysis of Benzene. V. Formation of Hot Benzene. *J. Chem. Phys.* **1982**, *77*, 6040–6050.

12 Sobolewski, A. L.; Woywod, C.; Domcke, W. Ab Initio Investigation of Potential-Energy Surfaces Involved in the Photophysics of Benzene and Pyrazine. *J. Chem. Phys.* **1993**, *98*, 5627–5641.

13 Lim, E. C. Photophysics of Gaseous Aromatic Molecules: Excess Vibrational Energy Dependence of Radiationless Processes. *Adv. Photochem.* **1997**, *23*, 165–211.

14 Lee, J.-K.; Zgierski, M. Z.; Lim, E. C. Unpublished results.

15 Fujiwara, T.; Lee, J.-K.; Zgierski, M. Z.; Lim, E. C. Photophysical and Spectroscopic Manifestations of the Low-Lying $\pi\sigma^*$ State of 4-(Dimethylamino)benzethyne:

Solvent-Polarity Dependence of Fluorescence and Excited-State Absorptions. *Phys. Chem. Chem. Phys.* **2009**, *11*, 2475–2479.

16 Chattopadhyay, N.; Serpa, C.; Pereira, M. M.; Seixas de Melo, J.; Arnaut, L. G.; Formosinho, S. J. Intramolecular Charge Transfer of *p*-(Dimethylamino)benzethyne: A Case of Nonfluorescent ICT State. *J. Phys. Chem. A* **2001**, *105*, 10025–10030.

17 Zachariasse, K. A.; Yoshihara, T.; Druzhinin, S. I. Picosecond and Nanosecond Fluorescence Decays of 4-(Dimethylamino)phenylacetylene in Comparison with those of 4-(Dimethylamino)benzonitrile. No Evidence for Intramolecular Charge Transfer and a Nonfluorescing Intramolecular Charge-Transfer State. *J. Phys. Chem. A* **2002**, *106*, 6325–6333, and references therein.

18 Zachariasse, K. A.; Grobys, M.; Tauer, E. Absence of Dual Fluorescence with 4-(Dimethylamino)phenylacetylene. A Comparison between Experimental Results and Theoretical Predictions. *Chem. Phys. Lett.* **1997**, *274*, 372–382.

19 Lippert, E.; Lüder, W.; Boos, H. In *Advances in Molecular Spectroscopy*; Mangini, A., Ed.; Pergamon: Oxford, U.K., 1962; pp 443−454.

20 Grabowski, Z. R.; Rotkiewicz, K.; Rettig, W. Structural Changes Accompanying Intramolecular Electron Transfer: Focus on Twisted Intramolecular Charge-Transfer States and Structures. *Chem. Rev.* **2003**, *103*, 3899–4032, and references therein.

21 Rotkiewicz, K.; Grellmann, K. H.; Grabowski, Z. R. Reinterpretation of the Anomalous Fluorescence of *p*-(Dimethylamino)benzonitrile. *Chem. Phys. Lett.* **1973**, *19*, 315–318.

22 Zachariasse, K. A.; Druzhinin, S. I.; Bosch, W.; Machinek, R. Intramolecular Charge Transfer with the Planarized 4-Aminobenzonitrile 1-*tert*-Butyl-6-cyano-1,2,3,4-tetrahydroquinoline (NTC6). *J. Am. Chem. Soc.* **2004**, *126*, 1705–1715.

23 For a comprehensive listing of theoretical work, see: Köhn, A.; Hättig, C. On the Nature of the Low-Lying Singlet States of 4-(Dimethylamino)benzonitrile. *J. Am. Chem. Soc.* **2004**, *126*, 7399–7410, and earlier references therein.

24 Hättig, C.; Hellweg, A.; Köhn, A. Intramolecular Charge-Transfer Mechanism in Quinolidines: The Role of the Amino Twist Angle. *J. Am. Chem. Soc.* **2006**, *128*, 15672–15682.

25 Gomez, I.; Mercier, Y.; Reguero, M. Theoretical Investigation of Luminescence Behavior as a Function of Alkyl Chain Size in 4-Aminobenzonitrile Alicyclic Derivatives. *J. Phys. Chem. A* **2006**, *110*, 11455–11461.

26 Druzhinin, S. I.; Ernsting, N. P.; Kovalenko, S. A.; Lustres, L. P.; Senyushkina, T. A.; Zachariasse, K. A. Dynamics of Ultrafast Intramolecular Charge Transfer with 4-(Dimethylamino)benzonitrile in Acetonitrile. *J. Phys. Chem. A* **2006**, *110*, 2955–2969, and references therein.

27 Zgierski, M. Z.; Lim, E. C. The Role of $\pi\sigma^*$ State in Intramolecular Electron-Transfer Dynamics of 4-Dimethylaminobenzonitrile and Related Molecules. *J. Chem. Phys.* **2004**, *121*, 2462–2465.

28 Zgierski, M. Z.; Lim, E. C. Electronic and Vibrational Spectra of the Low-Lying $\pi\sigma^*$ State of 4-Dimethylaminobenzonitrile: Comparison of Theoretical Predictions with Experiment. *J. Chem. Phys.* **2005**, *122*, 111103.

29 Campos Ramos, R.; Fujiwara, T.; Zgierski, M. Z.; Lim, E. C. Photophysics of Aromatic Molecules with Low-Lying $\pi\sigma^*$ States: Excitation-Energy Dependence of Fluorescence in Jet-Cooled Aromatic Nitriles. *J. Phys. Chem. A* **2005**, *109*, 7121–7126.

30 Druzhinin, S. I.; Demeter, A.; Galievsky, V. A.; Yoshihara, T.; Zachariasse, K. A. Thermally Activated Internal Conversion with 4-(Dimethylamino)benzonitrile, 4-(Methylamino)benzonitrile, and 4-Aminobenzonitrile in Alkane Solvents. No Correlation with Intramolecular Charge Transfer. *J. Phys. Chem. A* **2003**, *107*, 8075–8085.

31 Lee, J.-K.; Fujiwara, T.; Kofron, W. G.; Zgierski, M. Z.; Lim, E. C. The Low-Lying $\pi\sigma^*$ State and Its Role in the Intramolecular Charge Transfer of Aminobenzonitriles and Aminobenzethyne. *J. Chem. Phys.* **2008**, *128*, 164512.

32 Okada, T.; Mataga, N.; Baumann, W. $S_n \leftarrow S_1$ Absorption Spectra of 4-(*N,N*-Dimethylamino)benzonitrile in Various Solvents: Confirmation of the Intramolecular Ion Pair State in Polar Solvent. *J. Phys. Chem.* **1987**, *91*, 760–762.

33 Shida, T. *Electronic Absorption Spectra of Radical Ions*; Elsevier: Amsterdam, 1988.

34 Okada, T.; Uesugi, M.; Kohler, G.; Rechthaler, K.; Rotkiewicz, K.; Rettig, W.; Grabner, G. Time-Resolved Spectroscopy of DMABN and its Cage Derivatives 6-Cyanobenzoquinuclidine (CBQ) and Benzoquinuclidine (BQ). *Chem. Phys.* **1999**, *241*, 327–337.

35 Kwok, W. M.; Ma, C.; George, M. W.; Grills, D. C.; Matousek, P.; Parker, A. W.; Phillips, D.; Toner, W. T.; Towrie, M. Further Time-Resolved Spectroscopic Investigations on the Intramolecular Charge Transfer State of 4-Dimethylaminobenzonitrile (DMABN) and Its Derivatives, 4-Diethylaminobenzonitrile (DEABN) and 4-Dimethylamino-3,5-dimethylbenzonitrile (TMABN). *Phys. Chem. Chem. Phys.* **2003**, *5*, 1043–1050.

36 Gustavsson, T.; Coto, B. P.; Serrano-Andrés, L.; Fujiwara, T.; Lim, E. C. Do Fluorescence and Transient Absorption Probe the Same Intramolecular Charge Transfer State of 4-(Dimethylamino)benzonitrile? *J. Chem. Phys.* **2009**, *131*, 031101.

37 Coto, B. P.; Serrano-Andres, L.; Gustavsson, T.; Fujiwara, T.; Lim, E. C. manuscript in preparation.

38 Serrano-Andres, L.; Merchan, M.; Roos, B. O.; Lindh, R. Theoretical Study of the Internal Charge Transfer in Aminobenzonitriles. *J. Am. Chem. Soc.* **1995**, *117*, 3189–3204.

39 Zgierski, M. Z. Unpublished results.

40 Because of the triplet−triplet absorption with intensity maximum at 380 nm (Wang, Y. Quenching of Singlet and Triplet States of *p-N,N*-Dimethylaminobenzonitrile by Tertiary Amines. Intramolecular Charge-Transfer State and Excited-State Three-Electron Bond. *J. Chem. Soc., Faraday Trans. 2*, **1988**, 1809−1823), which strongly overlap the 420 nm TICT transient, it is very difficult to measure the decay time of the TICT state absorption at 420 nm.

41 Zgierski, M. Z.; Fujiwara, T.; Lim, E. C. Photophysics of Aromatic Molecules with Low-Lying $\pi\sigma^*$ states: Fluorinated Benzenes. *J. Chem. Phys.* **2005**, *122*, 144312.

42 Robin, M. B. *Higher Excited States of Polyatomic Molecules*; Academic Press: New York, 1975; Vol. III.

43 Frueholz, R. P.; Flicker, W. M.; Mosher, O. A.; Kuppermann, A. Electronic Spectroscopy of Benzene and the Fluorobenzenes by Variable Angle Electron Impact. *J. Chem. Phys.* **1979**, *70*, 3057–3070.

44 Philis, J.; Bolovinos, A.; Andritsopoulos, G.; Pantos, E.; Tsekeris, P. A Comparison of the Absorption Spectra of the Fluorobenzenes and Benzene in the Region 4.5−9.5 eV. *J. Phys. B* **1981**, *14*, 3621–3635.

45 Phillips, D. Fluorescence and Triplet State of Hexafluorobenzene. *J. Chem. Phys.* **1967**, *46*, 4679–4689.

46 Loper, G. L.; Lee, E. K. C. Fluorescence Decay and Radiative Lifetimes of Fluorinated Aromatic Molecules. *Chem. Phys. Lett.* **1972**, *13*, 140–143.

47 O'Connor, D. V.; Sumitani, M.; Morris, J. M.; Yoshihara, K. Non-exponential Picosecond Fluorescence Decay in Isolated Pentafluorobenzene and Hexafluorobenzene. *Chem. Phys. Lett.* **1982**, *93*, 350–354.

48 Kovalenko, S. A.; Dobryakov, A. L.; Farztdinov, V. Detecting Electronic Coherence in Excited-State Electron Transfer in Fluorinated Benzenes. *Phys. Rev. Lett.* **2006**, *96*, 068301.

49 Studzinski, H.; Zhang, S.; Wang, Y.; Temps, F. Ultrafast Nonradiative Dynamics in Electronically Excited Hexafluorobenzene by Femtosecond Time-Resolved Mass Spectrometry. *J. Chem. Phys.* **2008**, *128*, 164314.

50 Takemura, T.; Yamada, Y.; Sugawara, M.; Baba, H. A Kinetic Study of Dual Phosphorescence of Halogenated Benzenes in Rigid glass Solution. *J. Phys. Chem.* **1986**, *90*, 2324–2330.

51 Nagaoka, S.; Takemura, T.; Baba, H.; Koga, N.; Morokuma, K. Ab Initio Study on the Low-Lying Triplet State of Chlorobenzene. *J. Phys. Chem.* **1986**, *90*, 759–763.

52 Borg, O. A.; Liu, Y.-J.; Persson, P.; Lunell, S.; Karlsson, D.; Kadi, M.; Davidsson, J. Photochemistry of Bromofluorobenzenes. *J. Phys. Chem. A* **2006**, *110*, 7045–7056.